Comparison of Denver and Leeds laboratory flotation cells: Effect of particle size and hydrodynamics

by M.P. Tshazi[1], L.S. Leal Filho[2], N. Naude[1]

Affiliation:
[1]University of Pretoria, South Africa
[2]Universidade de São Paulo, Brazil

Correspondence to:
M.P. Tshazi

Email:
mfesane.tshazi@up.ac.za

Dates:
Received: 25 Aug. 2022
Revised: 29 Nov. 2024
Accepted: 27 Mar. 2025
Published: May 2025

How to cite:
Tshazi, M.P., Leal Filho, L.S., Naude, N. 2025. Comparison of Denver and Leeds laboratory flotation cells: Effect of particle size and hydrodynamics. *Journal of the Southern African Institute of Mining and Metallurgy*, vol. 125, no. 5, pp. 225–232

DOI ID:
https://doi.org/10.17159/2411-9717/2289/2025

ORCiD:
M.P. Tshazi
http://orcid.org/0009-0001-6389-1547
L.S. Leal Filho
http://orcid.org/0000-0001-8501-1857
N. Naude
http://orcid.org/0000-0002-9615-0243

Abstract

In this paper, the authors performed experiments in the Denver and Leeds laboratory flotation devices1 at the University of Pretoria at various particle sizes to evaluate the performance of the devices. Quartz was used in a single mineral system at discrete sizes fractions, -25 µm, +25-45 µm, +45-75 µm, and +75-106 µm. Hydrodynamic analysis, based on dimensionless power and Reynolds numbers, indicated that the Leeds cell required higher power input to achieve comparable flow conditions. Specifically, the Leeds cell exhibited an average power number of 1.03, whereas the Denver cell averaged 0.77 within the same impeller speed range of 1000 rpm–1500 rpm. For comparative flotation performance, impeller speeds were calibrated, resulting in operating speeds of 1200 rpm for the Denver cell and 1400 rpm for the Leeds cell. The cells performed similarly at two coarser-sized fractions. However, some deviations were observed in the finer particle size range. The -25 µm (fine) fraction initially achieved a recovery of only 15%. An additional reagent dosage was required to enhance the recovery of this fraction significantly. These findings highlighted the influence of particle size on flotation recovery. For all experiments, the Denver laboratory flotation cell outperformed (defined by higher recovery) the Leeds device, while still operating at a lower impeller speed. This advantage can be attributed to its impeller-stator design and air dispersion features, effectively overcoming slurry resistance and resulting in superior flotation performance compared to the Leeds cell.

Keywords

quartz, particle size, hydrodynamics, impeller speed, recovery

Introduction

Froth flotation

Froth flotation is commonly used to concentrate valuable minerals. This process depends on adequate surface exposure, i.e., the extent of liberation of the mineral, and selective hydrophobicity of the desired mineral(s). Froth flotation is regarded as a complex system, with many influencing factors and interdependent interactions. These factors and interactions are summarised as a flotation system, which is comprised of three categories of components namely: chemistry, equipment, and operation components. Each component is subdivided into many variables, such as particle size, collectors, and airflow, as shown in Figure 1. These flotation variables significantly influence flotation performance.

Laboratory flotation tests have made a considerable contribution to industrial process development and troubleshooting (Newcombe et al., 2012; Ross, 2019). The validity of correlation of laboratory batch froth flotation data to an industrial application is historically somewhat poor (Newcombe et al., 2012). This poor correlation has been linked to differences in equipment and operational variables between the laboratory and plant configurations.

A comparison of the Denver and Leeds laboratory cells was conducted over 40 years ago (Liddell, Dunne, 1984). However, the unique characteristics of these cells, like their structure, impeller, and air intake mechanism, were not explored. The study aimed to compare laboratory flotation cells, Denver and Leeds, across varying particle size ranges and hydrodynamic conditions to provide insight into how particle size and cell characteristics influence flotation performance under identical experimental conditions.

[1]All references to devices in this document refer to those used at the University of Pretoria.

Comparison of Denver and Leeds laboratory flotation cells: Effect of particle size

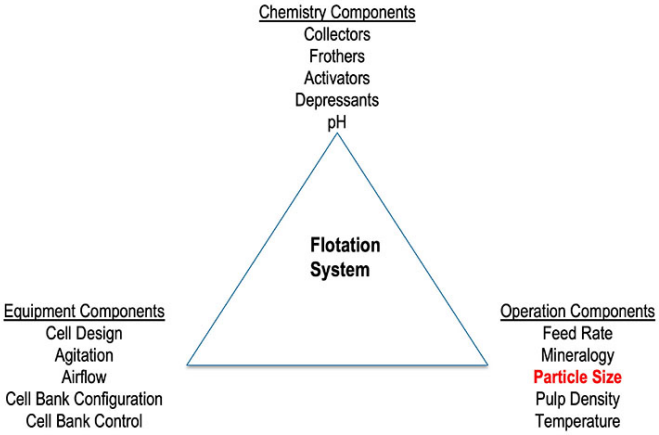

Figure 1—Various factors influencing a flotation system (Klimpel, 1984)

Figure 2 (left) illustrates a Denver D-12 laboratory flotation cell, which is widely used for conducting laboratory test work. Figure 2 (right) illustrates the Leeds laboratory flotation cell. As introduced by Professor C. Dell of the University of Leeds, this cell aimed to increase reproducibility of results and reduce operator-dependent factors. (Liddel, Dunne, 1983). Flotation tests performed in laboratories are usually dependent on the operator because froth scraping is generally done manually. The scraping areas of the

cells differ, with the Denver cell having the impeller in the centre, which obstructs scraping, while the Leeds cell has no obstruction. The Leeds cell features a froth crowder-like shape at the rear. The Leeds flotation cell is designed as a complete unit and parts are not easily interchangeable, whereas the Denver allows for much more flexibility as the cell size and/or impeller design can be changed easily without a significant redesign.

One of the biggest differences between the two cells is their impeller design (Figure 3): The Denver design has four equally sized holes from which the air is sheared as it is introduced into the cell; in the Leeds cell, air is introduced just above the impeller to be sheared. Some air is forced into the impeller and sheared to smaller equally sized bubbles, and some air bypasses the impeller to enter the cell. These differences cause different bubble flow patterns.

Mechanisms

In froth flotation, minerals are concentrated based on three main principles: true flotation, entrainment, entrapment, or a combination of these processes (Wills, Finch, 2015). True flotation is governed by three mechanisms: collision, attachment, and detachment. A brief description of true flotation is that a particle needs to collide with an air bubble, the two entities become attached, and then this unit must remain stable as it moves through the cell and into the froth zone until it is discharged via the cell lip. This is a chemically activated process (Wills, Finch, 2015). Entrainment is the result of water-suspended minerals deporting to the concentrate launder (Wang, 2016). The entrainment mechanism is non-selective as particles are not attached to air bubbles but are instead carried upward by the flow of water or by the wake created by bubble-particle aggregates (Smith, Warren, 1989). This mechanism can affect both valuable and gangue mineral particles. Wang et al. (2015) and Zheng et al. (2006) further observed that entrainment typically favours particle sizes below 50 µm, while entrapment occurs when minerals are trapped between air bubbles because of a non-draining froth phase. This mechanism primarily affects coarse particles (> 106 µm) more than fine particles (Zheng et al., 2006). Like entrainment, entrapment can concentrate both valuable and gangue minerals, leading to reduced selectivity in the flotation process.

Figure 2—Photographs of Denver (left) and Leeds (right) laboratory cells at the University of Pretoria

Figure 3—Impeller and stator configurations of the Denver (left and centre) and Leeds (right) laboratory cells

The floatability of a mineral is determined by its particle hydrophobicity (water repellence) and the hydrodynamic conditions that promote particle–bubble collisions, adhesion, and transport from the pulp to the froth. High floatability is typically observed in particles with large contact angles and high collection efficiency (E_k), which is expressed by Equation 1:

$$E_k = E_c E_a E_p, \quad [1]$$

where E_c is efficiency of particle–bubble collision; E_a is efficiency of adhesion; E_p is efficiency of preservation of the particle–bubble aggregate.

Particle size

In Trahar's (1981) study, it was highlighted that although particle size was recognised as a crucial factor in froth flotation, its practical advantages in the design and plant operations have been limited. This gap is expected to close to meet the challenges of processing increasingly complex ores. Particle size plays a crucial role in the efficiency of bubble-particle attachment (Rao, 2004), and flotation recovery is significantly influenced by the size of mineral particles (Jameson, 2012). Norori-McCormac et al. (2017) further demonstrated that even small changes in particle size distribution can significantly impact froths stability.

In addition to the influencing factors recorded in Figure 1, the effect of particle size on flotation recovery is highlighted in Figure 4, categorising particle sizes into three regions: fine, intermediate, and coarse. The specific boundaries of these regions depend on the mineral type and its properties. It is generally accepted that there is an ideal size range (intermediate) where recovery is maximised. Consequently, particles outside of a particular range will be compromised when floated and it is difficult to achieve optimum recoveries (Trahar, 1981).

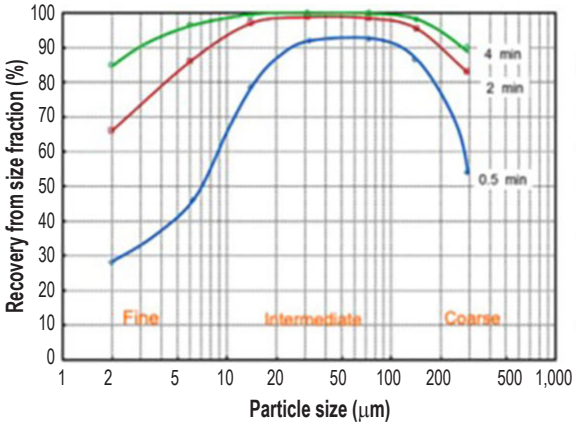

Figure 4—The effect of particle size on flotation recovery (Trahar, 1981)

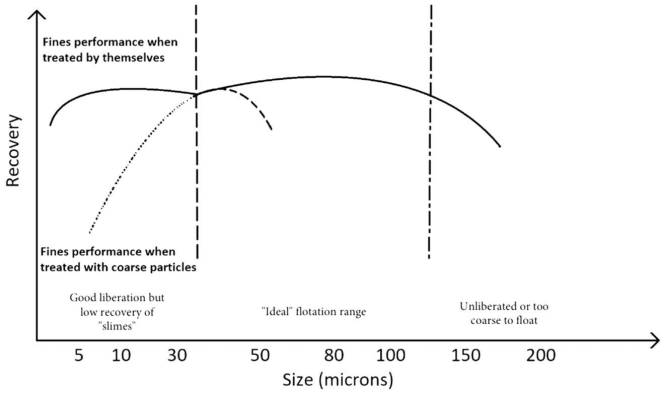

Figure 5—An illustration of recovery trend as a function of particle size in three regions, modified from Pease et al. (2006)

Pease et al. (2006), expounded on Trahar's findings, demonstrating the benefits of floating fine particles separately to maximize recovery (Figure 5). The study emphasised the importance of narrow size distribution in flotation operations, suggesting that both fine and coarse materials can be floated optimally if the kinetics associated with each size fraction are fully understood and controlled.

Fine particles suffer from poor collision efficiency, thus resulting in poor overall recovery (Nguyen, 2007; El-Rahiem, 2014). The main factors affecting this are bubble size, energy input, and pulp rheology, and therefore the recovery performance can be tuned by adjusting either one of those inputs. Moreover, due to the larger surface area of fine particles, higher reagent dosages are often required to render them hydrophobic (Pease et al., 2006). On the other hand, coarse particle flotation is decreased by the detachment of particles from bubbles (Wills, Finch, 2015). The main factors affecting this are hydrophobicity and energy input. Coarse particle recovery can be optimised by focusing on these inputs; however, it should be noted that fine and coarse particle recovery often react in an opposing manner (Safari et al., 2016). For instance, increasing energy input will benefit fine particle recovery while decreasing coarse particle recovery, and careful consideration should be used when optimising recovery of a certain size fraction.

Finer particles generally exhibit slower flotation rates compared to larger particles under conditions of low turbulent energy dissipation, as observed by Pyke et al. (2003). As a result Pyke et al. (2003) and Changunda et al. (2012), observed that kinetic rate (k) increases almost linearly with particle size. This phenomenon is related to the efficiency of particle-bubble collision.

Further research by Murhula, Hashan, and Otsuki (2022) demonstrated that flotation recovery is influenced by the interaction between solid concentration, particle size, and mineral type. In quartz flotation, for instance, higher recovery rates are typically achieved with higher solid concentrations and smaller particle size fractions, highlighting the role of entrainment, whereas more dilute pulps tend to enhance bubble loading efficiency while minimising entrainment (Ramlall, 2008).

Hydrodynamics

Hydrodynamics (fluid flow) within the flotation system are primarily influenced by the impeller (Shabalala et al., 2011; Souza Pinto et al., 2018). Hydrodynamic behaviour is typically characterised by hydrodynamic parameters and dimensionless numbers (Souza Pinto et al., 2018). These parameters and numbers account for the complex interactions and behaviours observed in the flotation system, as illustrated in Figure 1. Key dimensionless numbers include the power number (N_P), Reynolds number (N_{Re}), and Froude number (N_{Fr}), amongst others.

Dimensionless hydrodynamic numbers are valuable for benchmarking the performance of impellers and flotation cells (Rodrigues et al., 2001). Key dimensionless numbers, such as the N_{Re}, N_{Fr}, and N_P, are derived from operational variables (e.g., impeller rotational speed, volumetric airflow, pulp specific gravity, and dynamic viscosity) or geometric parameters (e.g., impeller diameter). These dimensionless numbers facilitate the analysis of fluid flow characteristics within a flotation cell. Table 1 provides a comprehensive summary of these parameters, including their formulas and typical ranges, enabling researchers to quickly assess fluid dynamics.

Table 1

Characterisation of flotation hydrodynamics with dimensionless numbers related to impeller characteristics (from Fuerstenau et al., 2007)

Number	Definition	Equation	Range	Description
Reynolds	$N_{Re} = \frac{ND^2\rho}{\mu}$	2	(1–7) x 10^6	Turbulence of fluid's intensity is reflected by this parameter (Wang, Liu, 2021)
Froude	$N_{Fr} = \frac{N^2D}{g}$	3	0.1–5	Describes solids suspension and characterisation of mixing intensity (Nelson, Lelinski, 2000)
Power	$N_P = \frac{P}{N^3D^5\rho}$	4	0.5–5	Describes dissipation and how the impeller draws power (Tabosa et al., 2016b)

where P is power drawn by impeller (W); N is impeller rotational speed (s^{-1}); D is impeller diameter (m); ρ is specific gravity (kg/m^3); μ is dynamic viscosity at a given temperature (kg/m.s); g is gravity acceleration (m/s^2).

N_P represents the net power drawn for both pumping and shearing, quantifying the resistance imposed by the slurry on the impeller blades, also known as the drag coefficient (C_D). A higher N_P signifies greater fluid displacement (Arbiter, Harris, 1962), which is advantageous for fine particles due to their low collision efficiency. N_P varies with the slurry flow regime and is typically plotted against the Reynolds number (N_{Re}), as shown in Figure 6. In laminar flow, NP decreases steadily, whereas in highly turbulent conditions ($N_{Re} > 10^4$), commonly observed in mechanical flotation cells, it remains constant (Harris, 1976; Harris, 1986; Leal Filho et al., 2002).

The dynamic viscosity of water at different temperatures is well-documented in literature. At 27°C, it is reported to be 0.8509 $\times 10^{-3}$ Pa·s (Ma et al., 2020). To estimate the dynamic viscosity of a slurry system, the Krieger–Dougherty Equation (5) is commonly used, particularly for monodisperse systems. The maximum packing fraction (φm) generally falls between 0.6 and 0.7, with a value of 0.63 often used for randomly packed spheres. Furthermore, for spherical particles, the intrinsic viscosity ([η]) is typically 2.5, as noted by Abo Dhaheer et al. (2015).

$$\frac{\mu}{\mu_0} = \left(1 - \frac{\varphi}{\varphi_m}\right)^{-[\eta]\varphi_m} \quad [5]$$

where μ and μ_0 are the dynamic viscosities of the slurry and water (Pa s), respectively; φ is volume fraction of the dispersed solid.

Experimental

Laboratory flotation cells

All tests were conducted using the Denver and Leeds laboratory flotation cells with nominal volumes of 3.5 L, both made of Perspex. Each cell was equipped with a distinct tachometer for adjusting the impeller speed. A centralised flow meter was employed to regulate the flow of air supplied from a compressed dry air cylinder, ensuring consistent and controlled aeration across the experiments. The Denver and Leeds cells had impeller diameters of 0.07 m and 0.074 m, respectively. The effect of particle size distribution was evaluated in the Denver and Leeds laboratory flotation cells, while maintaining all other variables (given in Figure 1) constant.

Experimental conditions and procedures

A 40 kg sample of 99.9% quartz was used. Quartz is classified as a strongly hydrophilic mineral (Wills, Finch, 2015) and therefore requires chemical activation. The material was wet-milled in a rod mill and thereafter wet-sieved to produce four narrow size fractions: –25 µm (fine), +25–45 µm (intermediate), +45–75 µm (medium), and +75–106 µm (coarse). Each fraction was separately blended and split with a rotary splitter to ensure that representative samples were used for the flotation tests. The cell operations were characterised in such a way that comparable kinetic results could be obtained. This was achieved by manually calibrating the impeller speeds of the cells, resulting in optimised speeds of 1200 rpm for the Denver cell and 1400 rpm for the Leeds cell. All tests were performed at 17 mass% solids in a 25 g/t Flotigam EDA ether amine collector, with a 2-minute conditioning time. This collector exhibits frothing properties and therefore no frother was added during the experiments. The pulp was adjusted to a pH of 9.5 with the aid of NaOH. An air flow of 2 L/min was employed. Three to four concentrates were collected every minute after manual scraping at a 10-second interval. It was necessary to conduct further tests on the –25 µm fraction at 50 and 175 g/t collector dosages of Flotigam EDA to improve recovery. Consequently, seven concentrates were collected from the higher collector dosed -25 µm fraction. In general, flotation continued until no froth was recoverable. The concentrates were filtered, oven dried, and weighed. All experiments were carried out repeatedly, with a variability limit of up to a maximum of 5% standard deviation.

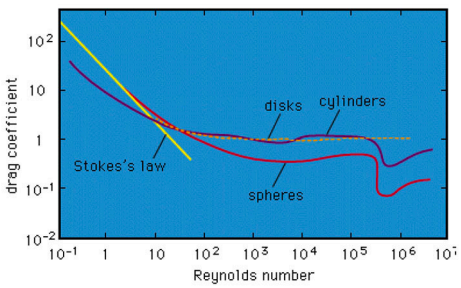

Figure 6—Drag coefficient (CD) as a function of flow regime (NRe) (Libii, 2010)

The power consumption of Denver and Leeds laboratory cells was measured using an Efergy Classic Wireless Energy Monitor. Tests were conducted at impeller speeds between 1000 rpm and 1500 rpm with increments of 1000 rpm. Testing was conducted under three conditions: an empty cell, a cell filled with 3 L of water with an air flow rate of 2 L/min, and a slurry mixture containing approximately 17 mass% quartz solids with an air flow rate of 2 L/min. The power draw was calculated by subtracting the power consumed under loaded conditions (water or slurry) from that recorded in the no-load (empty) condition.

Results and discussion

This section presents the results and discussions from a comparative study of Denver and Leeds cells at different particle size fractions. The study was conducted using a single mineral system, namely quartz, ensuring consistent mineralogy and resulting in uniform hydrophobicity.

Effect of particle size

The flotation of four particle size fractions was evaluated under optimised conditions. Figure 7 illustrates the average cumulative recoveries over time for the two larger size fractions: (medium) +45–75 µm, and (coarse) +75–106 µm. Both flotation cells performed similarly for the +45–75 µm fraction, achieving recoveries of approximately 80%. Whereas, for the +75–106 µm fraction, the Denver cell recorded a recovery of 74%, outperforming the Leeds cell by approximately 3%. The difference in performance between the two cells for the coarsest fraction could be attributed to the effect of turbulence, which is better dampened in the Denver cell compared to the Leeds cell. As a consequence of turbulence, which can disrupt particle–bubble aggregates, particularly when coarse particles are present, lower flotation efficiency is the result. (Yao et al., 2021). The recovery of both size fractions was completed within 2.5 minutes, which aligns with expectations, since these fractions fall mostly within the ideal flotation range of +25–106 µm (as shown in Figure 5). These recoveries were aided by the formation of stable and voluminous froths during flotation.

The kinetic constants were approximately the same for both cells for flotation of the intermediate (+45–75 µm) and coarse (+75–106 µm) size fractions, although the values for the Denver cell were slightly higher, aligning with the same trend as the recovery rates.

Comparison of Denver and Leeds laboratory flotation cells: Effect of particle size

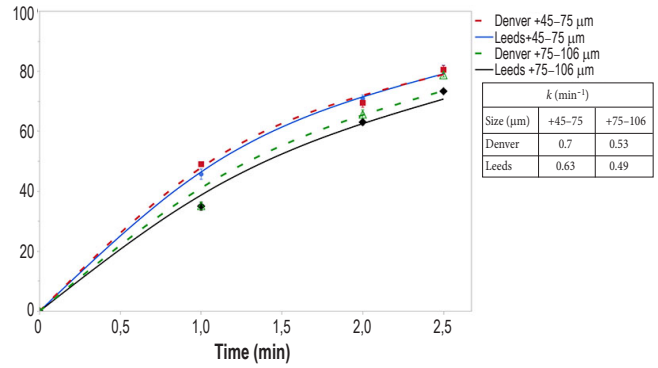

	k (min⁻¹)	
Size (µm)	+45–75	+75–106
Denver	0.7	0.53
Leeds	0.63	0.49

Figure 7—Comparison of Denver (dotted lines) and Leeds (solid lines) cells for kinetics curves for flotation of the medium (+45–75 µm and coarse (+75–106 µm) size fractions of silica, with corresponding rate constant in the legend label

Figure 8 presents the results for the smaller size fractions: fines (–25 µm) and intermediate (+25–45 µm). Recovery of the fine fraction (–25 µm) was very low for both cells, though the Denver cell achieved a slightly higher recovery of 15%. To support this, the Denver cell demonstrated nearly double the kinetic rate (0.32 min^{-1}) compared to the Leeds cell (0.18 min^{-1}), suggesting that the Denver impeller enhanced collision efficiency (E_c). The low recovery of the finest particles (–25 µm) can be largely attributed to the low collector dosage (25 g/t), which significantly hindered their flotation performance. Additionally, fines typically have a higher specific surface area (cm^2/g), leading to lower collision efficiencies between particles and bubbles. As Pease et al. (2006) showed, fines can achieve good flotation performance, but only when flotation conditions are specifically tailored to treat this fraction in a narrow size distribution range.

For the intermediate size fraction (+25–45 µm), the Denver cell outperformed the Leeds cell, with recoveries of 74% and 63%, respectively. This suggests that the Denver cell provided more favourable hydrodynamic conditions for particle–bubble collisions, a conclusion supported by the higher flotation rates of 0.65 min^{-1} for the Denver cell compared to 0.44 min^{-1} for the Leeds cell.

Moreover, both the fine (–25 µm) and intermediate (+25 –45 µm) size fractions required an additional 90 seconds to reach completion compared to the larger fractions. This finding is consistent with the conclusion of Pease et al. (2006) that finer particles generally require longer residence times in flotation processes than coarser particles.

The kinetic rate (k) was very low for the fine fraction (–25 µm) and increased with particle size, a trend consistent with the findings of Pyke et al. (2003) and Changuada et al. (2008). Particle size significantly affects the recovery rate, as highlighted by several researchers, including Trahar (1981), Rao (2004), and Jameson (2012). The maximum value of k was observed for the +45–75 µm fraction, but it decreased for the coarsest size fraction (+75 –106 µm). This behaviour can be attributed to the particle–bubble collection efficiency (E_k), which is determined by the product of collision efficiency (E_c), adhesion efficiency (E_a), and the preservation efficiency of the particle–bubble aggregate (E_p). Fine particles have low E_k due to poor E_c (i.e., limited particle–bubble collisions), while very coarse particles show reduced E_k because turbulence in the flotation cells tends to destroy the particle–bubble aggregates.

Pease et al. (2006) also demonstrated that finer particles require higher reagent dosages due to their larger specific surface area (cm^2/g). To improve the recovery of fines to levels comparable to those of the +25 µm size fractions, higher reagent dosages were investigated. The collector dosage was initially doubled, then further increased to 175 g/t. Figure 9 illustrates the impact of these increased dosages on fines recovery.

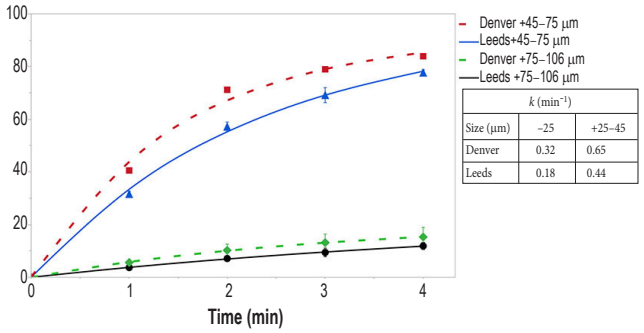

	k (min⁻¹)	
Size (µm)	–25	+25–45
Denver	0.32	0.65
Leeds	0.18	0.44

Figure 8—Comparison of Denver (dotted lines) and Leeds (solid lines) cells for kinetics curves for flotation of the intermediate (+25–45 µm) and fine (–25 µm) size fractions of silica, with corresponding rate constant in the legend label

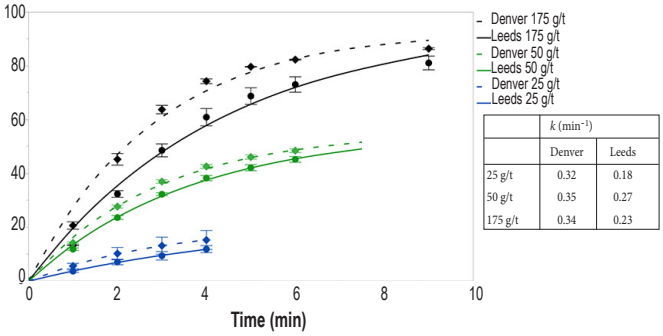

	k (min⁻¹)	
	Denver	Leeds
25 g/t	0.32	0.18
50 g/t	0.35	0.27
175 g/t	0.34	0.23

Figure 9—Effect of collector dosage on flotation recovery of fines (–25 µm) using the Denver (dotted lines) and Leeds (solid lines) cells, with corresponding rate constant in the legend label

Despite doubling the dosage, recovery levels still fell short of those achieved for the +25 µm fractions. However, when the dosage was raised to 175 g/t of Flotigam EDA, a significant improvement in flotation response was observed, with recovery levels becoming comparable to those of the larger size fractions. Also, notably so, this required up to nine minutes to reach completion. As previously mentioned, finer particles typically require longer flotation times. This increase in reagent dosage enhanced overall flotation rates and potentially contributed to greater particle stabilisation, resulting in higher fines recovery from the froth.

Despite a significant increase in reagent dosage for the finest size fraction (–25 µm), the average k values remained relatively low at 0.34 min^{-1} for the Denver cell and slightly lower at 0.23 min^{-1} for the Leeds cell. This suggests that the Leeds impeller was less effective in promoting particle–bubble collisions compared to the Denver impeller, as all other conditions were kept constant. The observed increase in recovery rates can be attributed to the higher reagent dosage, which aligns with the findings of Pease et al. (2006).

Hydrodynamic

Figure 10 presents the results for the water-only system, showing a general trend of decreasing power number with increasing Reynolds number. This aligns with Westhuizen's (2004) findings that the presence of air reduces the power number by decreasing the density effect around the impeller. The Leeds cell exhibited slightly higher turbulence intensities (higher Re) and power inputs than the Denver cell, except at 1000 rpm. Furthermore, increased turbulence

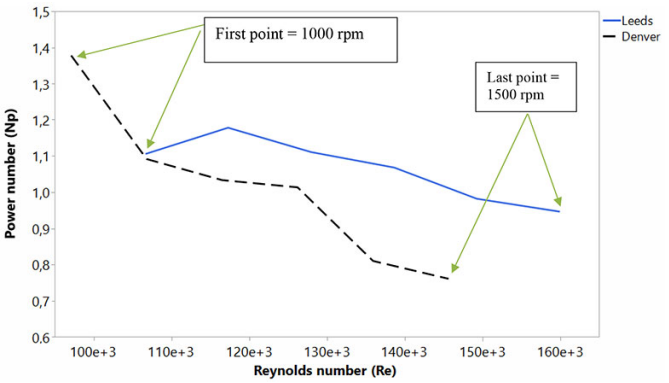

Figure 10—Power number vs. Reynolds number for water-air mixing in Denver and Leeds flotation cells

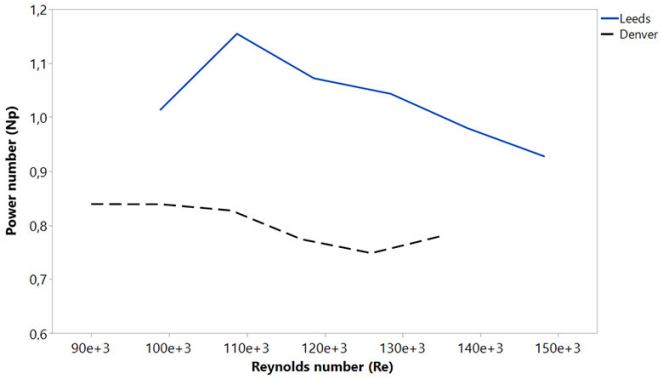

Figure 11—Power number vs. Reynolds number for quartz-water-air mixing in Denver and Leeds flotation cells between 1000 rpm and 1500 rpm

intensity (higher N_{Re}) and power input enhance bubble-particle collisions, especially for finer particles, leading to more efficient flotation, although excessive turbulence can potentially disrupt bubble-particle adhesion. These findings suggest that the Leeds cell is better suited for applications requiring higher turbulence intensity.

Figure 11 illustrates impeller performance in a slurry. The Leeds cell produced results similar to those in the water-only system, whereas the Denver cell maintained a stable power number of approximately 0.77 across the 1000 rpm–1500 rpm range. This stability highlights the Denver cell's ability to generate sufficient turbulence while consuming less power.

In the absence of solids (Figure 10), both cells operated in the transitional region between laminar and turbulent flow, as evidenced by fluctuations in power numbers, suggesting the presence of large eddy vortices. However, in slurry conditions (Figure 11), the Denver impeller demonstrated a greater ability to overcome resistance from solid particles, with its power number rapidly approaching the fully turbulent regime. In contrast, the Leeds impeller did not exhibit this behaviour under the experimental conditions. These results indicate that the Denver cell produced more consistent fluid fields while operating with greater power efficiency.

Additionally, the Denver and Leeds cells had similar Froude numbers ($2 < N_{Fr} < 4.5$ and $2.1 < N_{Fr} < 4.7$, respectively), indicating comparable solid suspension capabilities.

Conclusions

This study compared the performance of the Denver and Leeds laboratory flotation cells based on various particle size fractions and hydrodynamic characteristics to achieve comparable kinetic results.

Hydrodynamic characteristics included dimensionless numbers such as power and Reynolds numbers, which revealed that these cells require different operating conditions in the presence and absence of particles. Leeds demonstrated higher power numbers under both conditions, indicating greater resistance to movement imposed by water and slurry due to a unique impeller-stator design. As a result, the Leeds impeller must dissipate more power to facilitate particle and bubble dispersion and promote particle–bubble collisions.

Consequently, the cells needed to be operated at different rotational speeds, 1200 rpm for the Denver cell and 1400 rpm for the Leeds cell, to achieve similar performance. The difference in operating speeds required to obtain similar results can be linked to hydrodynamic characteristics, which influence the manner of air bubble creation in the cells and mineral recovery. These operating conditions were used for testing at narrow size fractions. The cells performed similarly at the coarser fractions, but there were some differences in the lower particle size range. This suggests that the impact of cell design, particularly impeller efficiency, becomes more pronounced at smaller particle sizes. The Denver cell reported higher recovery rates across all test ranges with faster kinetic rates.

The study emphasises the importance of cell design in flotation efficiency and highlights the critical role of particle size in flotation recovery. Fine particles require more reagents and longer flotation times (due to their larger surface area) to obtain optimum recoveries. Process efficiency will increase as a result of knowing how to optimise particle size distribution.

The results demonstrate that the Denver cell outperformed the Leeds cell, as the Leeds cell required a higher impeller speed to achieve similar recoveries. Overall, the Denver cell exhibited marginally superior performance, which can be attributed to its more versatile hydrodynamic characteristics, making it better suited for handling a broader range of particle sizes.

Acknowledgements

The authors wish to thank Anglo American for financial support and the University of Pretoria for use of the laboratory for this research. English editing of this manuscript was carried out by Prof. K. C. Sole.

References

Abo Dhaheer, M.S., Al-Rubaye, M.M., Alyhya, W.S., Karihaloo, B.L., Kulasegaram, S. 2015. Proportioning of self-compacting concrete mixes based on target plastic viscosity and compressive strength: part i - mix design procedure. *Journal of Sustainable Cement-Based Materials*, vol. 5, no. 4, 199–216. https://doi.org/10.1080/21650373.2015.1039625

Arbiter, N., Harris, C.C. 1962. Flotation machines. In: D.W. Fuerstenau (Editor). *Froth Flotation 50th Anniversary Volume*, Pap. 14. The American Institute of Mining, Metallurgical, and Petroleum Engineers, New York.

Changunda, K., Harris, M., Deglon, D.A. 2008. Investigating the effect of energy input on flotation kinetics in an oscillating grid flotation cell. *Minerals Engineering*, vol. 21, nos. 12–14, pp. 924–929. https://doi.org/10.1016/j.mineng.2008.03.015

El-Rahiem, F.H.A. 2014. Recent trends in flotation of fine particles. *Journal of Mining World Express*, vol. 3, pp. 63–79. https://doi.org/10.14355/mwe.2014.03.009

Fuerstenau, M.C., Jameson, G.J., Yoon, R. H. 2007. *Froth flotation: a century of innovation*. Littleton, Colo.: Society for Mining, Metallurgy, and Exploration.

Harris, C.C. 1976. Flotation machines. In: Fuerstenau, M.C. Flotation: A.M. Gaudin Memorial Volume. AIME, New York, vol. 2, p. 788.

Harris, C.C. 1986. Flotation machines design, scale up and performance: data base. In: Somasundaran, P. (ed), Advances in mineral processing. Symposium honoring Nathaniel Arbiter on his 75th birthday, New Orleans. Littleton, p. 618–635.

Jameson, G.J. 2012. The effect of surface liberation and particle size on flotation rate constants. *Minerals Engineering*, 36-38, pp. 132–137. https://doi.org/10.1016/j.mineng.2012.03.011

Klimpel, R.R. 1984. Use of chemical reagents in flotation. *Chemical Engineering*, vol. 91, no. 18, pp. 75–79.

Leal Filho, L.S., Rodrigues, W.J., Ralston, J. 2002. Importance of hydrodynamics in coarse particle flotation. In: Ralston, J., Miller, J., Rubio, J. (eds). Flotation and flocculation: from fundamentals to applications. Snap Printing, Medindie (Australia), p. 203-212.

Libii, J.N. 2010. Using wind tunnel tests to study pressure distributions around a bluff body: the case of a circular cylinder.

Liddel, K.S., Dunne, R C. 1983. An evaluation of the Leeds laboratory-scale flotation cell. Council for Mineral Technology (Mintek), Randburg, South Africa.

Ma, Y., Li, S., Zhang, L., Li, H., Liu, Z. 2020. Numerical simulation on heat extraction performance of enhanced geothermal system under the different well layout. *Energy Exploration & Exploitation*, vol. 38, no. 1, pp. 274–297. https://doi.org/10.1177/0144598719880350

Murhula, E., Hashan, M., Otsuki, A. 2022. Effect of Solid Concentration and Particle Size on the Flotation Kinetics and Entrainment of Quartz and Hematite. *Metals*. vol. 13, no. 53, pp. 1–21. https://doi.org/10.3390/met13010053

Nelson, M.G., Lelinski, D. 2000. 'Hydrodynamic Design of Self-Aerating Flotation Machines', Minerals Engineering, 13(10), 991–998. doi:10.1016/S0892- 6875(00)00085- 6

Newcombe, B., Bradshaw, D., Wightman, E. 2012. Development of a laboratory method to predict plant flash flotation performance. *Minerals Engineering*, vol. 39, pp. 228–238. https://doi.org/10.1016/j.mineng.2012.07.008

Nguyen, A.V. 2007. Flotation, Encyclopedia of Separation Science, pp. 1–27. https://doi.org/10.1016/B0-12-226770-2/00071-5

Norori-McCormac, A., Brito-Parada, P.R., Hadler, K., Cole, K., Cilliers, J.J. 2017. The effect of particle size distribution on froth stability in flotation. *Separation and Purification Technology*, vol. 184, pp. 240–247. https://doi.org/10.1016/j.seppur.2017.04.022

Pease, J.D., Curry, D.C., Young, M.F. 2006. Designing Flotation Circuits for High Fines Recovery. *Minerals Engineering*, vol. 19, no. 6, pp. 831–840. doi:10.1016/j.mineng.2005.09.056

Pyke, B., Fornasiero, D., Ralston, J. 2003. Bubble particle heterocoagulation under turbulent conditions. *Journal of Colloid and Interface Science*, vol. 265, no. 1, pp. 141–151. https://doi.org/10.1016/S0021-9797(03)00345-X

Ramlall, N.V. 2008. Development and modelling of a semi-batch. dissertation.

Rao, S.R. 2004. Flotation Kinetics and Fine Particle Flotation. In: *Surface Chemistry of Froth Flotation*. Springer, Boston, MA. https://doi.org/10.1007/978-1-4757-4302-9_14

Rodrigues, W.J., Leal Filho, L.S., Masini, E.A. 2001. Hydrodynamic Dimensionless Parameters and Their Influence on Flotation Performance of Coarse Particles. *Minerals Engineering*, vol. 14, no. 9, pp. 1047–1054. doi:10.1016/S0892-6875(01)00110-8

Ross, V. 2019. Key aspects of bench flotation as a geometallurgical characterization tool. *Journal of the Southern African Institute of Mining and Metallurgy*, vol. 119, no. 4, pp. 361–367. https://doi.org/10.17159/2411-9717/605/2019

Shabalala, N.Z.P., Harris, M., Leal Filho, L.S., Deglon, D.A. 2011. Effect of slurry rheology on gas dispersion in a pilot-scale mechanical flotation cell. *Minerals Engineering*, vol. 24, no. 13, pp. 1448–1453. https://doi.org/10.1016/j.mineng.2011.07.004

Safari, M., Harris, M., Deglon, D., Leal Filho, L., Testa, F. 2016. The effect of energy input on flotation kinetics. *International Journal of Mineral Processing*, vol. 156, pp. 108–115. https://doi.org/10.1016/j.minpro.2016.05.008

Smith, P.G., Warren, L.J. 1989. Entrainment of Particles into Flotation Froths. *Mineral Processing and Extractive Metallurgy Review*, vol. 5, nos. 1–4, pp. 123–145. https://doi.org/10.1080/08827508908952647

Souza Pinto, T.C., Braga, A.S., Leal Filho, L.S., Deglon, D.A. 2018. Analysis of key mixing parameters in industrial wemco mechanical flotation cells. *Minerals Engineering*, vol. 123, pp. 167–172. https://doi.org/10.1016/j.mineng.2018.03.046

Tabosa, E., Runge, K., Holtham, P., Duffy, K. 2016. Improving flotation energy efficiency by optimizing cell hydrodynamics. *Minerals Engineering*, vol. 96–97, pp. 194–202. https://doi.org/10.1016/j.mineng.2016.05.002

Trahar, W.J. 1981. A rational interpretation of the role of particle size in flotation. *International Journal of Mineral Processing*, vol. 8, no. 4, pp. 289–327. https://doi.org/10.1016/0301-7516(81)90019-3

Wang, L. 2016. Entrainment of fine particles in froth flotation, Thesis: Doctor of Philosophy, University of Queensland, Australia.

Wang, D., Liu, Q. 2021. Hydrodynamics of Froth Flotation and Its Effects on Fine and Ultrafine Mineral Particle Flotation: A Literature Review. *Minerals Engineering*, vol. 173. doi:10.1016/j.mineng.2021.107220

Westhuizen, A.P.P. 2004. The evaluation of solids suspension in a pilot scale mechanical flotation cell. Master dissertation. University of Cape Town, Cape Town, page 25.

Wills, B.A., Finch, J.A. 2015. Wills' Mineral Processing Technology: An Introduction to the Practical Aspects of Ore Treatment and Mineral Recovery. 8th edn., Oxford: Butterworth-Heinemann.

Yao, N., Liu, J., Sun, X., Liu, Y., Chen, S., Wang, G. 2021. A Rational Interpretation of the Role of Turbulence in Particle-Bubble Interactions. *Minerals*, vol. 11, no. 9, p. 1006. https://doi.org/10.3390/min11091006

Zheng, X., Johnson, N.W., Franzidis, J.-P. 2006. Modelling of Entrainment in Industrial Flotation Cells: Water Recovery and Degree of Entrainment. *Minerals Engineering*, vol. 19, no. 11, pp. 1191–1203. doi:10.1016/j.mineng.2005.11.005 ◆

GIW® MDX = BEST IN CLASS MILL CIRCUIT PUMP

★★★★★

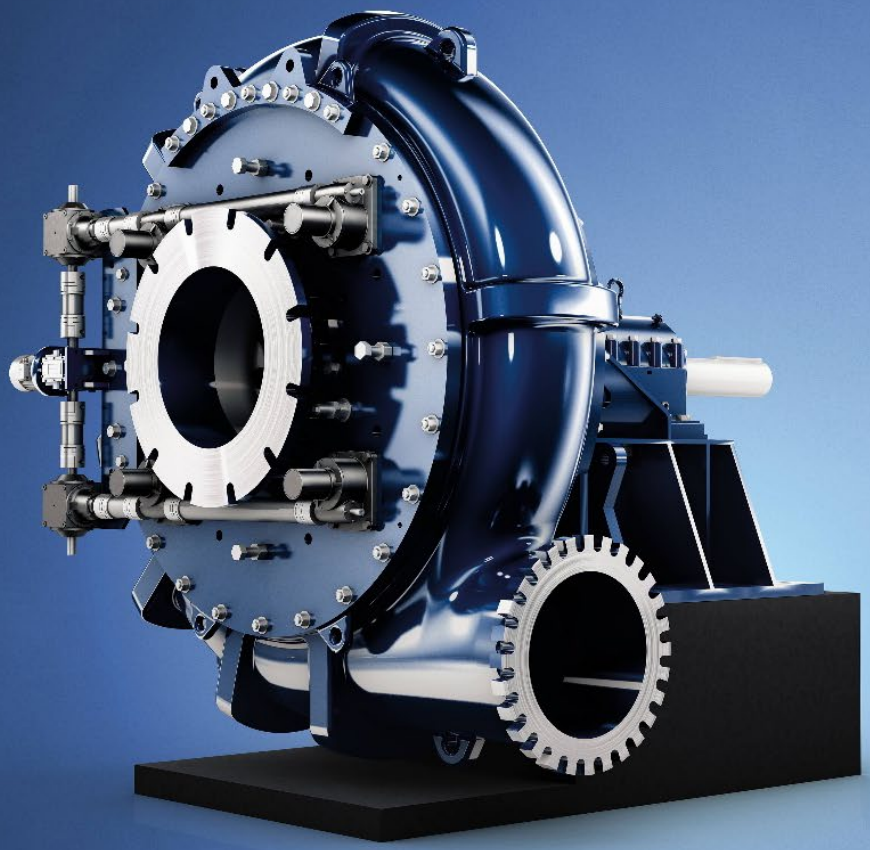

Best In Class Pumps for Aggressive Slurries

Mining operators are seeing an increased demand for minerals and ores. Operators must now consider the costs of pump maintenance and replacement as well as the cost-benefit of utilizing fewer larger pumps versus several smaller pumps to perform the same work.

The KSB GIW® MDX pump line delivers proven results in the harshest hard rock mining applications.

KSB MINING

W: www.ksb.com/en-za
T: +27-11-876-5600

KSB